International Journal of Thermodynamics (IJoT)
ISSN 1301-9724 / e-ISSN 2146-1511
https://dergipark.org.tr/en/pub/ijot

Vol. 27 (No. 1), pp. 001-012, 2024
doi: 10.5541/ijot.1272871
Published online: March 1, 2024

Research Article

Effects of Nozzle Diameter and Holes Number on the Performance and Emissions of a Gasoline Direct Injection Engine

[1]*O. M. Yousif, [2]M. A. Mashkour

[1]Mechanical Engineering Department, University of Technology -Iraq
[2]Mechanical Engineering Department, University of Technology -Iraq
E-mails: [1]*21980@student.uotechnology.edu.iq, [2]Mahmoud.A.Mashkour@uotechnology.edu.iq

Received 29 March 2023, Revised 27 June 2023, Accepted 27 September 2023

Abstract

The goal of the current study is to estimate how a gasoline direct injection (GDI) engine's performance and emissions are affected by the fuel injector nozzle diameter and hole number of its injectors. A thermodynamic mathematical modelling has been created utilizing a software program written in the MATLAB language to simulate the two-zone combustion process of a four-stroke direct injection engine running on gasoline at (Rotation Engine Speed 3000 revolution per minute (rpm), 40 MPa injection pressure, compression ratio 9.5, and spark timing 145°). The first law of thermodynamics, equation of energy, mass conserving, equation of state, and mass fraction burned were all used in the creation of the software program. The study was carried out at five different nozzle diameters (0.250, 0.350, 0.450, 0.550, and 0.650 mm) and nozzle hole numbers (4,6,8,10,12). The results show that the GDI engine's performance and emissions are significantly influenced by variations in nozzle hole diameter and number. It was shown that engine power, heat transfer, cylinder pressure, and temperature increased with increasing nozzle hole diameter and number of nozzle holes and the maximum value was seen with nozzle hole diameter 0.650 mm and (12) holes. The lowest value for the nozzle hole diameter and number of holes was found to be 0.250 mm and 4 nozzle holes, which resulted in the lowest emissions of carbon monoxide CO and nitrogen monoxide NO. The study was also conducted for different operating conditions (Rotation Engine speed of 1000, 2000, 3000, 4000, 5000 rpm ,35 MPa injection pressure , compression ratio of 11.5 , and spark timing of 140°) and the same nozzle diameters and nozzle holes number mentioned previously to estimate the maximum values for temperature, pressure, power , heat transfer and emissions . The results of the second part of the study showed that the highest of maximum values of temperature, pressure, and emissions were at of 1000 rpm, a nozzle diameter of 0.650 mm, and (12) holes. The highest values for maximum power at 4000 rpm, a nozzle diameter of 0.650 mm and (12) holes, while the highest maximum values for heat transfer are at 5000 rpm, a diameter of 0.65mm and (12) holes.

Keywords: *Gasoline direct injection engine (GDI); nozzle diameter; hole number; mathematical model; performance; emissions.*

1.Introduction

(GDI) engine technology has sparked considerable interest in recent years due to its several advantages over traditional fuel injection (PFI) engines, including reduced fuel consumption, improved efficiency, and lower hazardous emissions to comply with environmental requirements[1] , [2]. Although GDI engines provide rapid reaction and flexible control, several aspects impact engine performance and engine emissions, including ignition and injection timings, injection pressure, injection duration, diameter of nozzles, and aperture numbers, among others .Studying combustion engines experimentally is a very challenging issue because of the sophisticated experimental facilities that are required to perform the experiments. Therefore, researchers tend to perform theoretical or analytical analyses such as simulation and numerical analysis before conducting any experimental activity.

Cost and time may be saved by using a simulation approach that enables GDI engine designers to adjust and examine a variety of factors with no need to actually create any real part or even an entire engine. Numerous mathematical models, including combustion phasing modeling, thermophysical property models, injector models, and flow models into and out of a cylinder engine, have been developed to aid in understanding, correlating, and investigating the process of engine cycles [3].

The impact of engine settings on a DI engine's performance and emission characteristics has been examined in several studies related to diesel and gasoline. Kumbhar *et al*. [4] used computation fluid dynamics CFD codes with a combustion model to test four different nozzle throat diameters and their influence upon the engine performance, emissions, as well as spraying features. They discovered that improvements in spray cone angle, fuel atomization, and effective air-fuel mixture resulted to a 0.230 mm nozzle throat diameter, which led to the highest in-cylinder temperatures and pressures. Hydrocarbon (HC), Carbon monoxide (CO), and soot emission got decreased as nozzle hole diameter dropped; nevertheless, Nitric oxide (NO) emissions were reported to rise because of improved

*Corresponding Author

atomizing as well as a general increase within cylinder gas temperatures of nozzle holes by smaller sizes. As a result, nozzle throats having smaller diameters have a tendency to lower emission at the cost of increased NOx emission. Lee *et al.* [5] investigated the development of fuel spray-air mixing, combustion, and emitting as the number of injector throats changed. The researchers found that there is a optimal number of holes for better efficiency and emission of the diesel engine. Furthermore, the findings demonstrate that evaporating, atomizing, and combustion are significantly impacted by the amount of holes present. On the other hand, when the number of injector holes exceeds a certain limit, the combustion and emissions deteriorate as a result of an absence of air entraining necessary to create a stoichiometric mixture. By using a flux dynamometer, a four-stroke single-cylinder diesel engine, a water-cooled direct injection diesel engine operated by computer, a typical injection timescale of 23° before top dead center (BTDC), and a variety of throat diameters, Kumar *et al.* [6] studied the performance, combustion, and emitting of the engine for the different nozzles hole dimension (3 holes × Ø = 0.20 mm), (3 holes × Ø = 0.28 mm) and (3 holes × Ø = 0.20 mm) as shown in figure 1. The results of this study showed that among all different nozzle throats, the 3 holes × Ø = 0.20 mm (adapted) improved the time. The findings were outstanding in terms of performance, combustion, and emitting. The only disadvantage was that NOx numbers rise when the aperture nozzle hole size is reduced.

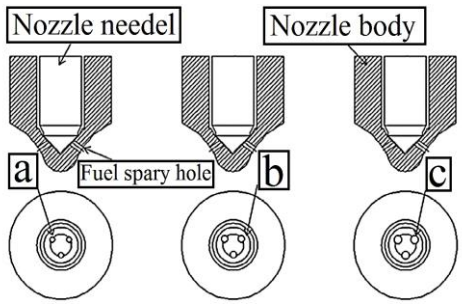

Figure 1. Schematic drawing of 3-holes of different nozzle diameters(a) Ø = 0.20 mm, (b) Ø = 0.28mm, (c) Ø =0.31mm.

Jiang C and Parker M., *et al.* [7] studied the influence of injection nozzle design upon the (GDI) engine fuel spray features. Inside a pressure- and temperature-controlled constant volume chamber as well as outside, testing on two custom three-hole injectors were carried out. The measuring was made at intervals of 15 mm, 25 mm, and 40 mm from the injection tip, radially outwards from the injection axis to the external edge of the jet. The researchers found that the spray penetration length before collapsing is determined by the injection pressure rise within extending such length. To understand the performance during flash boiling circumstances, average velocity and droplet diameter information were also studied. Additionally, the results showed that droplet size decreases whereas droplet velocity greatly rises during flash boiling circumstances. Researchers discovered that various hole geometries had distinct effects on sprays when exposed to a flash boiling setting. Some hole configurations provide more protection from spray collapsing. The researchers discovered that the spray produced by the middle of the three-hole sizes studied dispersed more easily than the spray produced by either smaller and greater hole diameters. Moreover, the convergent hole was more likely to show spray collapsing during flash boiling circumstances. Ahmed and Mekonen [8] conducted a simulation study by using ANSYS the influence of different injector nozzle hole numbers (INHNs) and fuel injection pressures (IPs) of the performance, and emissions characteristics of engine .The study performed for different fuel IPs 190, 200, 210, and 220 bar with a change of INHN of 1 (default), 3, and 4), each 0.84, 0.33, and 0.25 mm in orifice diameter , respectively as showing in figure 2 .The results show the increasing of INHNs and fuel IPs have an essential improvement of atomization and mixing rates, as well as combustion and engine efficiency as well as minimize of CO and HC emissions with a small raise in NOx .

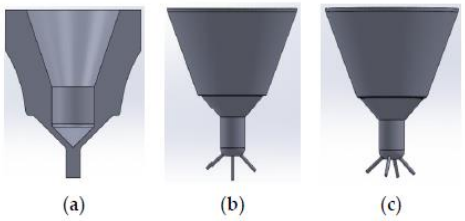

Figure 2. A diagram of fluid in nozzles: (a) single hole, (b) 3-holes, (c) 4-holes.

Reddy and Mallikarjuna [9] studied the impact of fuel injection settings on the performance, combustion, and emitting features of GDI engines by using CFD. For a variety of fuel injection pressures, spark timing, holes number, and multiple stage injection strategies, turbulence, combustion, and fuel spraying break-up analyses were carried out. The findings demonstrate that, relative to 110-bar fuel injection pressure, soot emission decreased for various fuel injection pressures by roughly 77.8 and 88.5% for 150 and 200-bar fuel injection pressures, respectively. When spark timing was advanced, the soot emission rose by an amount that was about 3.3 and 4.5 orders of magnitude more, correspondingly, at the spark time of 15° and 20° BTDC than at the spark time of 7.5° BTDC. Additionally, relative to a 6-hole injection, the soot emission is lower when 8 or 10 fuel injection holes were employed. The soot emission dropped by around 72.8 and 76.1%, correspondingly, in comparison to single-stage fuel injection, when two different multiple stage fuel injection techniques were taken into account. Eventually, it was determined that a GDI engine's preparing of the mixture and soot emission are significantly influenced by the fuel injection pressure, amount of injection holes, spark time, and multiple stage fuel injection technique. Employing (CFD) research and information from literatures, Jadhav and Mallikarjuna [10] investigated the impact of fuel injection-hole diameter and fuel injection time upon the mix formation in a four-stroke, wall-guided GDI type of engines. GDI engine at a compression ratio of 11.5. CFD simulating is run at an engine velocity of 2000 revs per minute. Three crank angle measures, three fuel injection times, as well as three fuel injection hole sizes of 0.1, 0.14, and 0.18 mm were used. The findings demonstrate that larger nozzle-hole diameters produced extremely rich mixing zones close to the spark plug. Furthermore, a greater suggested mean effective pressure was seen with a smaller nozzle-hole diameter and delayed fuel injection time.

According to the preceding discussion, numerous researchers have concentrated on various elements of engine parameters of GDI engines utilizing various approaches and

techniques. The injector setting effect upon the performance as well as emitting characteristics of a GDI engine, on the other hand, has not been well examined. As a result, the present work aims at using MATLAB to investigate such effect. This work will be useful in enhancing the GDI engine settings for optimal performance.

2. Theoretical Model

This model examines a direct injection engine. The model depends on a two-zone thermodynamic study of the combustion process, which separates the combustion chamber into burned and unburned areas. The ideal gas law is assumed for the in-cylinder gases, and the first law of thermodynamics, state equation, and mass and volume conservation are used. For the temperature, pressure, mass, and volume of the burned and unburned gases, a set of equations may be constructed. The Wiebe function has the following definition. [11]:

$$X_{b(\theta)}=1\text{-}\exp\left[-a\left[\frac{\theta_{(i)}-\theta_{(0)}}{\theta_{(b)}}\right]^{k+1}\right] \quad (1)$$

where $\Theta(i)$ represents the immediate crank angle, $\Theta(o)$ represents the spark angle at the beginning of combustion, and $\Theta(b)$ represents the combustion duration. The values of a and k represent adjustable constants (5 and 2 are typical values). The burn profile is engine-specific, and the constants a and k can be changed on a specific engine or application since the burn profile is engine-specific.

The following equation is created by differentiating the ideal gas equation of state:

$$\frac{dp}{d\theta}=\left(-\frac{P}{V}\right)\left(\frac{dV}{d\theta}\right)+\left(\frac{P}{T}\right)\left(\frac{dT}{d\theta}\right) \quad (2)$$

In which the instantaneous quantities P, V, T, are modeled in relation to the crank angle of the engine. The first law of thermodynamics, which has the following formal formulation, may be implemented using the same procedure:

$$\Delta U=Q\text{-}W \quad (3)$$

Here Q represents the overall heat input into the system, W represents the work output from the system, and U represents the change in internal energy inside the system. Equation 4 may be produced by diffusing "Eq. (3)" [11]:

$$\frac{dU}{d\theta}=\left(\frac{dQ}{d\theta}\right)-\left(\frac{dW}{d\theta}\right)=mC_v\left(\frac{dT}{d\theta}\right) \quad (4)$$

Here C_v denotes the specific heat of the gas in the combustion chamber. The change in temperature as a function of crank angle is given by "Eq. (5)", which we get at by dividing the specific heat by the universal gas constant, utilizing Ŋ (the combustion efficiency), and L.H.V. (the lower heating values of the provided fuel):

$$\frac{dT}{d\theta}=T(\gamma\text{-}1)\left[\left(\frac{1}{PV}\right)\left(\frac{dQ}{d\theta}\right)-\left(\frac{1}{V}\right)\left(\frac{dV}{d\theta}\right)\right] \quad (5)$$

The changing in pressure as a product of the crank angle may be determined using the heat input from the fuel. The definition of the fuel's heat input is [12]:

$$Q_{in}=\eta_c\,.\mathrm{LHV}\left(\frac{1}{\mathrm{AF_{ac}}}\right)\left(\frac{P}{RT}\right)\mathrm{V_d} \quad (6)$$

In which the actual air-fuel rate is Q_{in} in. The final definition of the pressure change would be:

$$\frac{dP}{d\theta}=\left(\frac{-\gamma P}{V}\right)\left(\frac{dV}{d\theta}\right)+\left(\frac{\gamma\text{-}1}{V}\right)Q_{in}\frac{dX_b}{d\theta}+(\gamma\text{-}1)\left(\frac{1}{V}\right)\left(\frac{dQ_w}{d\theta}\right) \quad (7)$$

"Eq. (7)" serves as the foundation for a numeric model that mimics engine performance.

2.1 Modeling Engine Friction

The Several studies, notably Heywood [11] and Blair [13], have used general linear equations to forecast Friction mean effective pressure FMEP loses like a function of rpm. Although this approach only offers rough estimates of friction loses, it serves as a starting point for a numerical simulation. The following is Blair's equation for the linear FMEP loss:

$$FMEP=\mathrm{a}+\mathrm{b}(L)(RPM) \quad (8)$$

In which L represents the engine's stroke [m], rpm represents the engine speed [rev/min], while a and b represent constants that depend on the type of engine. According to the engine displacement, Blair has aspired to several variations of the FMEP loss equations for a spark-ignition engine with simple internal bearings($(V_d > 500\ cm^3)$ *and* $(V_d < 500\ cm^3)$ respectively :

$$FMEP=100000+350(L)(RPM) \quad (8a)$$

$$\mathrm{FMEP}=100000+100(500-V_d)+350(L)(\mathrm{RPM}) \quad (8b)$$

The indicated, relative FMEP losses are given in [Pa] units.

2.2 Burned and Unburned Areas

Assumptions must be made regarding the burned and unburned areas because this model ignores heat transmission between the burned and unburned zones and doesn't explore the geometric location of the flame front. The definitions of the unburned and burned zones are given in Rakopoulos and Michos' article [14]:

$$A_u(i)=A(i)\left(1\text{-}(X_b(i))^{\frac{1}{2}}\right) \quad (9)$$

$$A_b(i)=A(i)\left(\frac{X_b(i)}{(X_b(i))^{\frac{1}{2}}}\right) \quad (10)$$

The mass fraction burned like a function of crank angle gets denoted by *Xb*. The area of the cylinder that is now in touch with combustion chamber gases is known as A(i).

Although this technique ignores heat transmission between zones and presupposes a surface area of the cylinder head, it could be demonstrated to have physical consistency because the fractional heat transfer between the burned gas and the cylinder wall has always been greater in the burned region [18].

2.3 Burned, Unburned Mass, Volume, Temperature Calculations

The equation of state can be applied to the unburned and burned gas regions at any instant:

$$PV_b=m_bR_bT_b \quad (11a)$$

$$PV_u = m_u R_u T_u \quad (11b)$$

For the assumption of no mass loss from the combustion chamber, the total mass in the system at any stage can be expressed as:

$$m = m_b + m_u \quad (12)$$

The total volume at any stage

$$V = V_b + V_u \quad (13)$$

These are the main equations used; at any instant during combustion, there are seven unknown parameters to be solved ($T_b, T_u, m_b, m_u, V_b, V_u, P$). In order to solve these parameters, an extra equation that specifies the burning rate is required. In the simple form of the model, the burning rate can be expressed by the exponential form of Wiebe function "Eq. (1)",

2.4 Heat Transfer Estimation

The main modes of heat transfer from each zone are convection and radiation, this heat is determined using relationships based on the work of Annand [15]. Nusselt and Reynolds number correlations for forced convection are:

$$Nu_i = 0.94\, Re^{0.7} \quad (14)$$

The coefficient of radiation heat transferring is calculated as:

$$hr = 4.25 * 10^{-9} * \left(\frac{T^4 - T_w^4}{T - T_w}\right) \quad (15)$$

Convective losses into the wall are calculated as a function of the crank angle as follows:

$$DQ_1 = (hg(i) + hr(i)) A_b(i)(T_b(i) - T_w) * \frac{60}{360 * RPM} + (hg(i) + hr(i)) A_u(i)(T_u(i) - T_w) * \frac{60}{360 * RPM} \quad (16)$$

Calculates change in heat transfer (total) as A function of crank angle

$$DQ_2 = \eta * m_f * \text{L.H.V} * Dx_i - DQ_1 \quad (17)$$

2.5 Injector Calculations

Fuel velocity in model accounts as follows [16]:

$$U_{fuel} = \frac{C_d}{C_a} \sqrt{\frac{2 * (P_{inj} - P) * 1000}{\rho_{fuel}}} \left(\frac{m}{s}\right) \quad (18)$$

The following is accounted for by mass flow ratio in kilograms per millisecond:

$$\dot{m}_f = C_a A_{inj} \rho_f U_f \text{(kg/s)} \quad (19)$$

The following is how mass flow rate per crank angle unit is calculated:

$$\dot{m}_{CA} = \frac{holes * \dot{m}_f}{0.006 * N_s * MW_f} \left(\frac{kmol}{deg}\right) \quad (20)$$

Crank angle unit injection duration is calculated as follows:

$$dur_{CA} = \frac{m_f}{\dot{m}_{CA}} \text{ (deg)} \quad (21)$$

The following relationship is accounted for by the pressure injection for each time step:

$$P_{inj} = P_{injmin} + \left(\frac{P_{injmax} - P_{injmin}}{dur_{CA}}\right) * \theta \quad (22)$$

Where, $Pinj_{max}$ is maximum injection pressure, $Pinj_{min}$ is minimum injection pressure, and θ is crank angle.

2.6 Power, Torque, and Efficiency Calculations

The power is represented by the braking power *Wb*, and the engine torque τ, represents the amount of work completed per unit revolution (radians) of the crank [12].

$$\dot{W}_b = 2\pi \tau N \quad (23)$$

The network transmitted from the gas to the piston throughout a cycle is the stated work W_i , that represents the integration of the pressure over the cylinder volume.

$$W_i = \int P dV \quad (24)$$

while the designated power W_i , for any engine using η_c cylinders, is

$$\dot{W}_i = \eta_c W_i N/2 \quad (25)$$

Mechanical efficiency η_m is determined by the braking power to indicate power rate:

$$\eta_m = \frac{\dot{W}_b}{\dot{W}_i} \quad (26)$$

2.7 The Combustion Reaction (Equilibrium Equations) [17]

$$C a H_b O_c N_d + \frac{a_s}{\phi}(O_2 + 3.76 N_2) \longrightarrow n_1 CO_2 + n_2 H_2O + n_3 N_2 + n_4 O_2 + n_5 CO + n_6 H_2 + n_7 H + n_8 O + n_9 OH + n_{10} NO \quad (27)$$

Where a_s and ϕ are stoichiometric air--fuel ratio and equivalence ratio. The following four formulas are produced via atom balance:

$$C: \; a = (y_1 + y_5) N$$

$$H: \; b = (2y_2 + 2y_6 + y_7 + y_9) N$$

$$O: \; c + \frac{2a_s}{\phi} = (2y_1 + y_2 + 2y_4 + y_5 + y_8 + y_9 + y_{10}) N$$

$$N: \; d + 7.52 a_s/\phi = (2y_3 + y_{10}) N \quad (28)$$

where N stands for moles' total number. By definition, the mole fractions sum to 1:

$$\sum_{i=1}^{10} y_i = 1 \quad (29)$$

These equations define the following three constants:

$$d_1 = \frac{b}{a}, \quad d_2 = \frac{c}{a} + 2\frac{a_s}{\phi a}, \quad d_3 = \frac{d}{a} + \frac{7.52 a_s}{\phi a} \quad (30)$$

After some rearranging and replacement into the atom balancing equations, we have:

$$2y_1+2y_6+y_7+y_9+d_1y_1-d_1y_5=0$$

$$2y_2+y_2+2\,y_4+y_5+y_8+y_9+y_{10}-d_2y_1-d_2y_5=0$$

$$2y_3+y_{10}-d_3y_1-d_3y_5=0$$

$$\sum y_i=1 \qquad (31)$$

Six gas-phase equilibrium processes are now shown. Such reactions result in the creation of OH and NO as well as the dissociating of hydrogen, oxygen, water, and carbon dioxide:

$$\frac{1}{2}H_2 \leftrightarrows H \quad K_1=\frac{y_7 P^{\frac{1}{2}}}{y_6^{\frac{1}{2}}}$$

$$\frac{1}{2}O_2 \leftrightarrows O \quad K_2=\frac{y_8 P^{\frac{1}{2}}}{y_4^{\frac{1}{2}}}$$

$$\frac{1}{2}H_2+\frac{1}{2}O_2 \leftrightarrows OH \quad K_3=\frac{y_9}{y_4^{\frac{1}{2}} y_6^{\frac{1}{2}}}$$

$$\frac{1}{2}O_2+\frac{1}{2}N_2 \leftrightarrows NO \quad K_4=\frac{y_{10}}{y_4^{\frac{1}{2}} y_3^{\frac{1}{2}}}$$

$$H_2+\frac{1}{2}O_2 \leftrightarrows H_2O \quad K_5=\frac{y_2}{y_4^{\frac{1}{2}} y_6 P^{\frac{1}{2}}}$$

$$CO+\frac{1}{2}O_2 \leftrightarrows CO2 \quad K_6=\frac{y_1}{y_4^{\frac{1}{2}} y_5 P^{\frac{1}{2}}} \qquad (32)$$

The equilibrium constants had been curve-fit to the JANAF Table data for the temperature range 600 T > 4000 K by Olikara and Borman [18]. Their expressions take the following form:

$$log_{10}K_i(T)=A_i\, ln\left(\frac{T}{1000}\right)+\frac{B_i}{T}+C_i+D_iT+E_iT^2 \qquad (33)$$

Where T is the temperature in kelvin, and $(A_i, B_i, C_i, D_i, E_i)$ are the curve-fitting equilibrium constants. The unburned and burned mixed zones are regarded as independent open systems according to thermal characteristics. The atom balance equations are changed to correspond to the six separate equilibrium reacting equations, resulting in four equations with four unknowns (y_3, y_4, y_5, y_6). Such four equations have numerical solutions.

2.8 Variable Specific Heats Ratio Model

For combustion processes including iso-octane and other fuels, Krieger and Borman created this polynomial approach in 1966 [19]. The Krieger and Borman technique simulates changes in internal energy by using "correction factors" for ideal gas constants that correlate to temperature variations (based on a given reference temperature). Using this approach and the related polynomials, it is possible to derive the exact heats rate as a temperature function.

3. MATLAB Model

Figure 3 illustrates the flow chart of the model's mathematical formulation. Sub-models are created by the primary model to carry out certain tasks. The mathematical model's structure is as follows,

The piston's isentropic compressing and expanding in the cylinder are simulated by the isentropic sub-model. This model calculates the thermodynamic properties of cylinder in each step, which is theta equal 1 of crank angle degree, in piston movement according to the isentropic relation and by employing the engine geometry relations.

3.1 Injection sub-model

It replicates the processes of fuel injection and association, such as combustion, heat release, and heat transfer. This model, which is regarded as the most significant model, includes a number of sub-models for the injector, fuel characteristics, heat releasing and transmission, and ignition delay.

3.2 Equilibrium Sub-Model

In this model, the mole fraction of the combustion products and their specifications are calculated. The general algorithm of this model is shown in figure 4. The equilibrium model comprises several sub-models, such as minimum step $fmin$ sub-model, guess sub-model, newton sub-model, and line search sub-model.

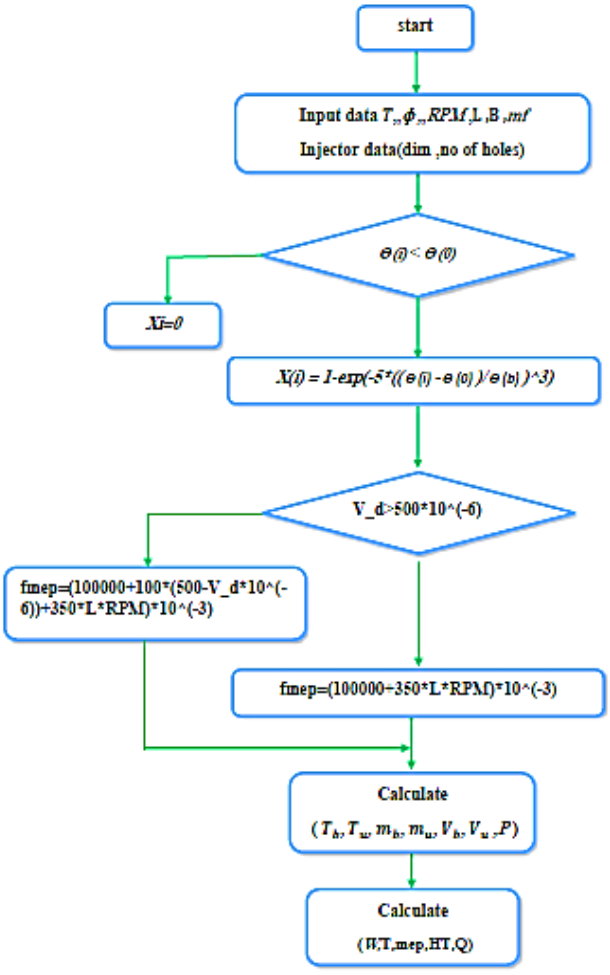

Figure 3. Algorithm of Main Model.

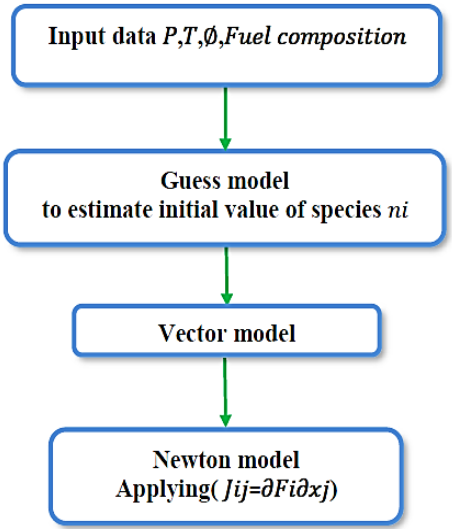

Figure.4 Algorithm of Equilibrium Model.

4. Results and Discussion

4.1Validation of the Matlab Model

Figure 5 shows the comparison of in-cylinder pressures obtained from the present Matlab Model and CFD simulation results of [Reddy A. et al., 9] for holes number 8 and compression ratio 9.3. From Figure 3, It can be observed that, there is a reasonably good agreement among the results. Therefore, the models used in this Matlab Model are working well and therefore they can be used with confidence for further study.

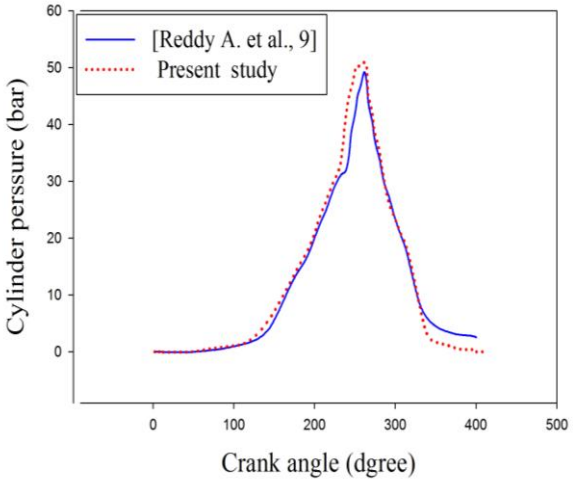

Figure 5. Comparison of in-cylinder pressures.

4.2 Variation of Orifice Diameter

The mathematical model for a GDI engine at (3000 rpm and 40 MPa injection pressure and compression ratio 9.5 spark timing 145°) is shown in Figure 6 the influence of nozzle hole diameter on the variation of cylinder pressure with crank angle. Increasing the hole diameter led to increase the cylinder pressure, as it can be observed. The maximum value of in-cylinder pressure is at the nozzle hole with a diameter of 0.650 mm due to due to the increase in injection area, which led to an increasing within fuel mass flow rate and quantity of heat release.

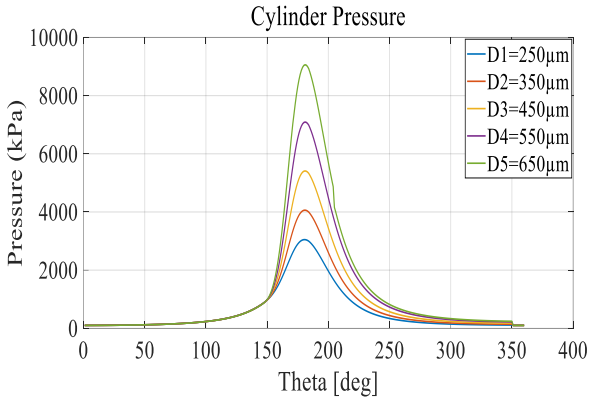

Figure 6. Cylinder pressure for different hole diameters.

The impact of nozzle hole diameter on the changing burned and unburned gas temperatures with crank angle is shown in figure 7. Although the impact of hole width on unburned gas temperature is minimal, it has a significant influence on burned temperature. By increased the diameter of the nozzle as it can be noticed, the burned gas temperature also increased. The 0.650 mm diameter nozzle hole produced a greater in-cylinder gas temperature due to the increased injection area, increased fuel mass flow rate, and increased heat release.

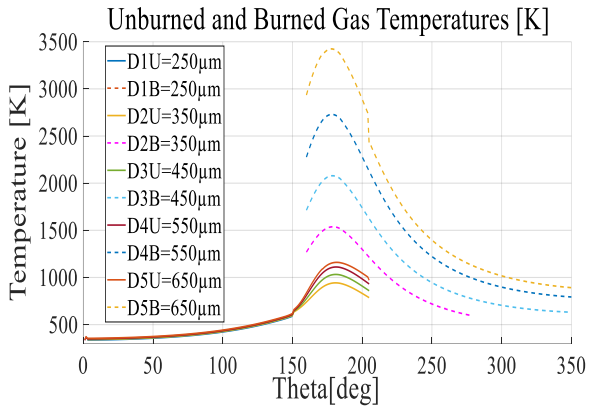

Figure 7. burned and unburned gas temperature for different hole diameters.

Figures 8 and 9 depict the impact of hole diameter on engine power and heat transfer as a function of crank angle. By increment the diameter of the nozzle as it can be observed, the engine power and heat transfer also increase because of the increased gas pressure brought on by an increase in the injection area, which leads to increase the fuel mass flow rate and heat release.

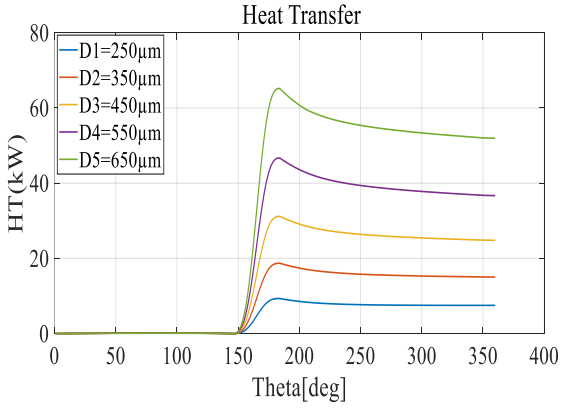

Figure.8 Engine power for different hole diameters.

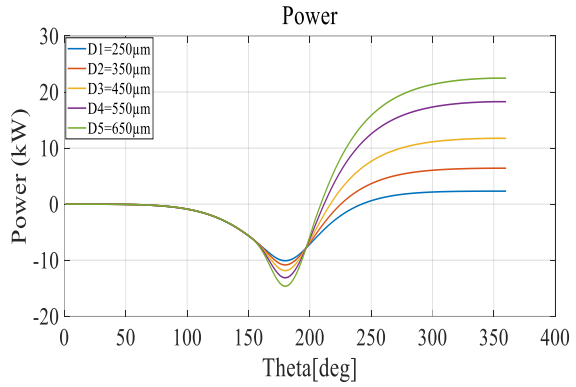

Figure 9. Heat transfer for different hole diameters.

Figure 10 shows CO emissions, as a function of crank angle at various fuel injector nozzle-hole sizes. These emissions of CO rise as the diameter of the nozzle hole increases. This is due to the fact that local rich zones begin to form as the injection area and fuel mass flow rate increase.

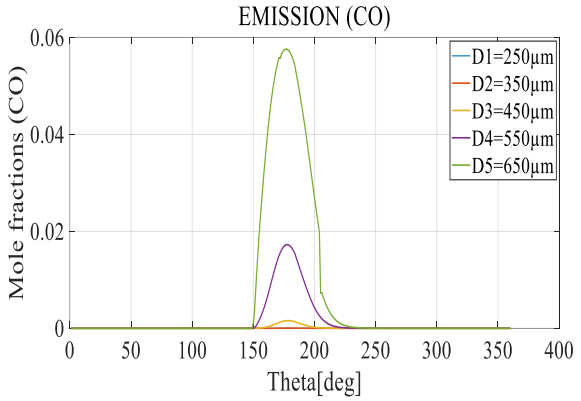

Figure.10. Effect of hole diameter on emissions of CO.

Figure 11 depicts NO emissions as a function of crank at various fuel injector nozzle-hole sizes. It is observed that the NO emissions rise as the diameter of the nozzle hole grows. This is due to the fact that bigger nozzle-hole sizes led to rich mixture and then higher in-cylinder temperatures.

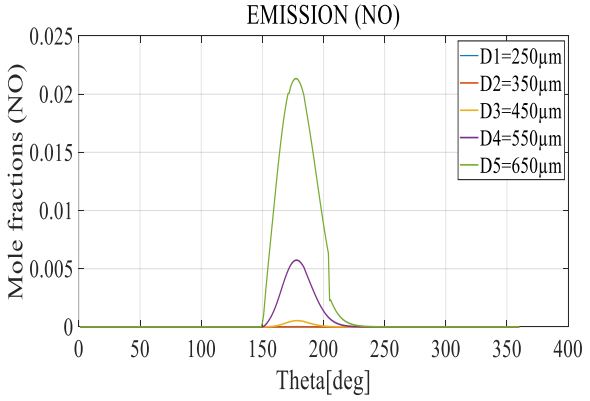

Figure.11. Effect of hole diameter on emissions of NO.

Figures 12 and 13 demonstrate the greatest power per cycle and optimal nozzle diameter vs. engine compression ratio as the number of holes is varied. It was shown that the greatest engine power per cycle was attained when the nozzle diameter (0.630 mm) and compression ratio (11) with (6) holes number were used.

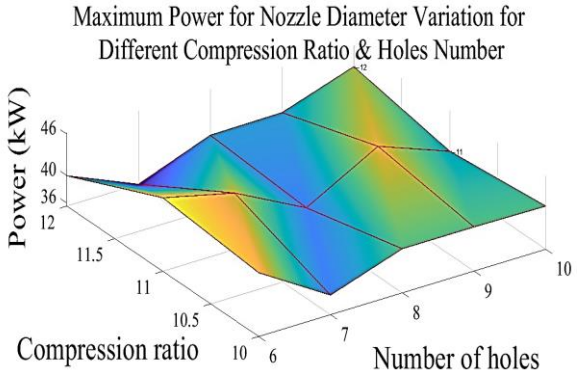

Figure 12. Maximum power for nozzle diameter variation for different compression ratio & holes number.

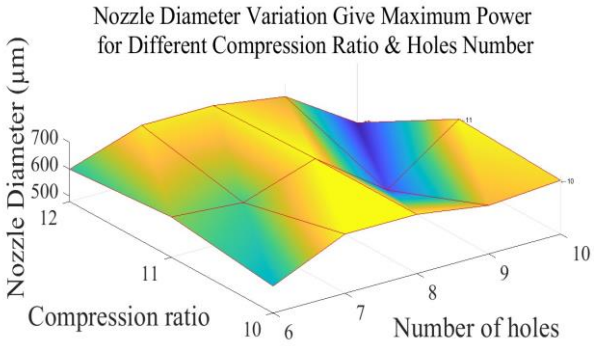

Figure 13. Nozzle diameter variation give maximum power for different compression ratio & holes number.

4.3 Variation of Orifice Diameter with Rotation Engine Speed.

Data in the table 1show the influence of the variation of nozzle hole diameter on the maximum values for temperature, pressure, power, heat transfer and emissions. The mathematical model for a GDI engine at (Rotation Engine speed of 1000, 2000, 3000, 4000, 5000 rpm ,35 MPa injection pressure, compression ratio of 11.5, and spark timing of 140°). The highest of maximum values of temperature, pressure, and emissions were at a 1000 rpm and diameter of 0.650 mm. The highest values for maximum power at 4000 rpm and nozzle diameter of 0.650 mm, while the highest maximum values for heat transfer are at 5000 rpm and diameter of 0.65mm.

4.4 Variation of the Number of Nozzle Holes

Figure 14 shows the effect of injector holes' number on the variation in-cylinder pressure with crank angle as determined by the mathematical model for the GDI engine at (3000 rpm, 40 MPa injection pressure, compression ratio 9.5, and spark timing 145°) by using the MATLAB software. Because of the regular distribution of equivalence ratios throughout the spark plug area, it is observed that when the fuel injector holes' number rises, the in-cylinder pressure also rises. This is due to the creation of excellent fuel droplets with an increasing within the fuel injector holes number.

Figure 15 depicts the influence of hole number on burned and unburned gas temperatures as a function of crank angle. The influence of hole number on unburned temperature is minimal, whereas the hole number influence upon burned gas temperature is significant. By increased the injector holes number as it can be noticed, the burned gas temperature also increased. and highest gas temperature among the others at (12) nozzle holes number.

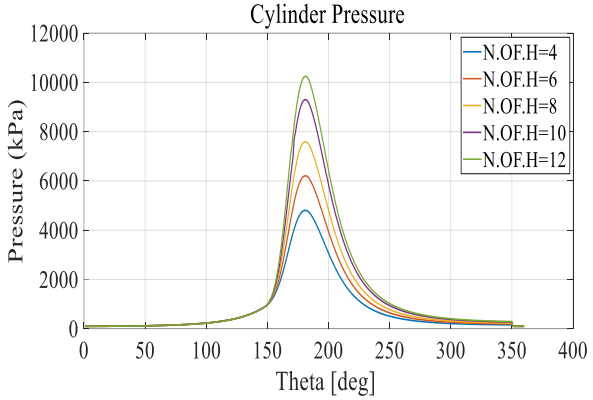

Figure 14. Cylinder pressure for different holes number.

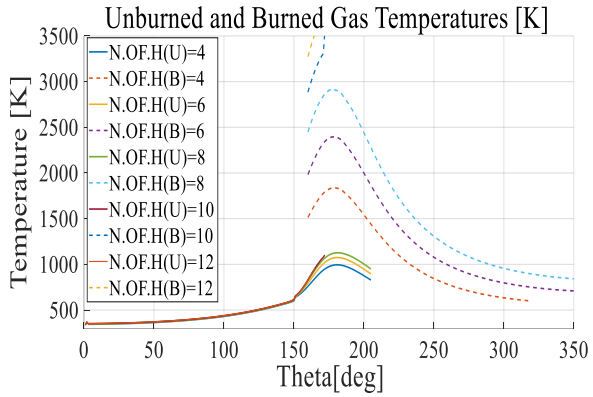

Figure15. Burned and unburned gas temperature for different holes number.

Table 1. Variation of Maximum Values of Operating Engine Parameters with Nozzle Diameter.

Temperature(K)

	Speed (rpm)				
D(mm)	1000	2000	3000	4000	5000
0.25	1767	1789	1536	1356	1124
0.35	1916	1921	1754	1527	1343
0.45	2467	2671	2224	1734	1542
0.55	2976	2987	2685	2223	1936
0.65	3187	3165	3013	2775	2430

Pressure (kPa)

	Speed (rpm)				
D(mm)	1000	2000	3000	4000	5000
0.25	5284	4471	3852	3541	3354
0.35	7331	6300	5088	4474	4103
0.45	8974	7724	6729	5715	5102
0.55	9750	8654	7773	6563	6028
0.65	10674	9476	8537	7663	6940

Power (kW)

	Speed (rpm)				
D(mm)	1000	2000	3000	4000	5000
0.25	2.261	1.807	1.183	0.5134	0.3456
0.35	4.918	5.051	4.639	4.095	3.492
0.45	7.667	9.19	9.118	8.767	8.296
0.55	11.48	13.34	14.56	14.48	14.19
0.65	11.35	20.92	21.38	24.84	21.16

Heat transfer (kW)

	Speed (rpm)				
D(mm)	1000	2000	3000	4000	5000
0.25	8.643	8.991	9.352	9.793	10.04
0.35	17	17.35	17.42	17.8	18.39
0.45	27.79	28.8	29.05	30.16	30.97
0.55	37.54	42.85	43.53	44.79	45.93
0.65	52.36	59.07	60.72	61.17	63.56

Mole fraction of CO (*Xi*)

	Speed (rpm)				
D(mm)	1000	2000	3000	4000	5000
0.25	6.1 e-04	2.3 e-07	1.47e-06	1.8 e-6	7.53e-07
0.35	0.02874	6.24 e-04	3.47e-05	6.33 e-06	8.53e-06
0.45	0.07289	0.01387	0.00132	1.83 e-07	3.63e-05
0.55	0.08544	0.053	0.01437	0.002918	0.00068
0.65	0.1582	0.07495	0.05509	0.03227	0.00592

Mole fraction of NO(*Xi*)

	Speed (rpm)				
D(mm)	1000	2000	3000	4000	5000
0.25	0.00021	3.61 e-06	7.74e-06	4.79e-07	4.49e-07
0.35	0.00989	0.000222	1.37e-05	3.88e-06	3.88e-06
0.45	0.02439	0.004718	0.00046	6.79E-05	1.44e-05
0.55	0.03021	0.01895	0.00489	0.001002	0.00024
0.65	0.03976	0.0258	0.02021	0.01134	0.00201

Figures 16 and 17 demonstrate impact of nozzle hole number on engine power and heat transfer as a function of crank angle. we can notice as the number of holes rise, so does engine power and heat transfer. This is due to increase in-cylinder pressures, as well as better atomization and a faster heat transfer rate.

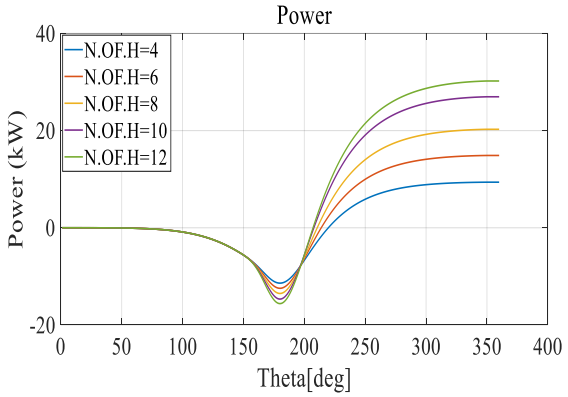

Figure.16. Engine power for different holes numbers.

The CO emissions are shown in Figure 18 at different fuel injector nozzle-hole numeral as a function of the crank angle. We can see that as the of nozzle-holes increase, so do the amount of CO emissions. This is because increased injection area and subsequent rise in fuel mass flow rate that result in local rich zones and dissociation of combustion products at high temperatures.

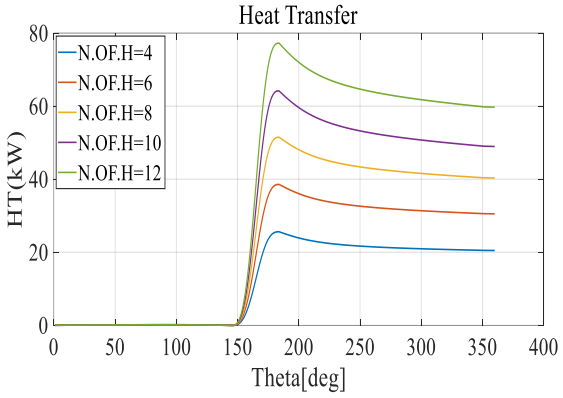

Figure.17. Heat transfer for different hole numbers.

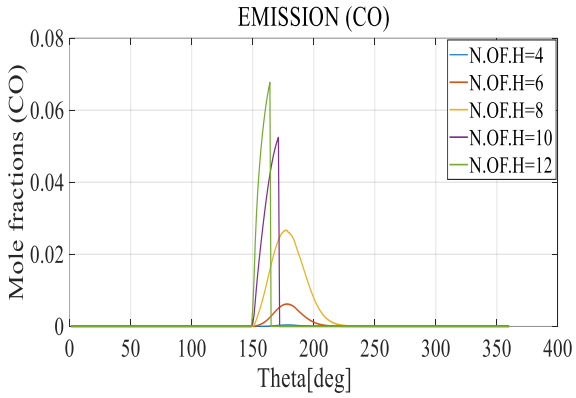

Figure18. Effect of holes number on emissions of CO.

Figure 19 explain NO emissions as a function of crank at various fuel injector nozzle-hole numeral. We can observe that NO emissions increase with increase in nozzle holes number. This is because the generation of NO is known to be significantly influenced by the thermal NO mechanism, which is extremely dependent on the temperature and the environment inside the cylinder. Higher numbers of nozzle holes result rich mixture zone and then higher in-cylinder temperature.

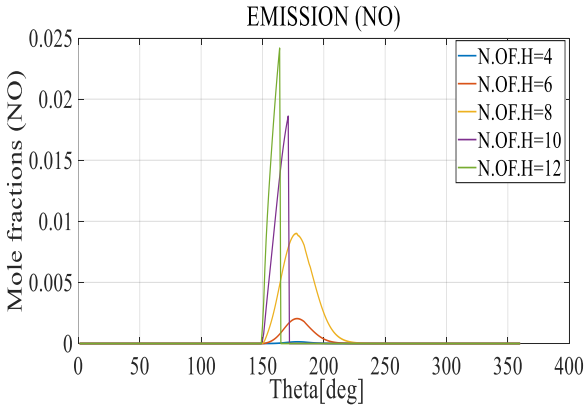

Figure.19. Effect of holes number on emissions of NO.

Figures (20) and (21) show the maximum power per cycle and the ideal number of nozzle holes in relation to engine compression ratio and nozzle diameter change. Figure 18 shows that the highest power per cycle generated at nozzle diameter (0.450 mm), the number of holes is (14) and the compression ratio is (12).

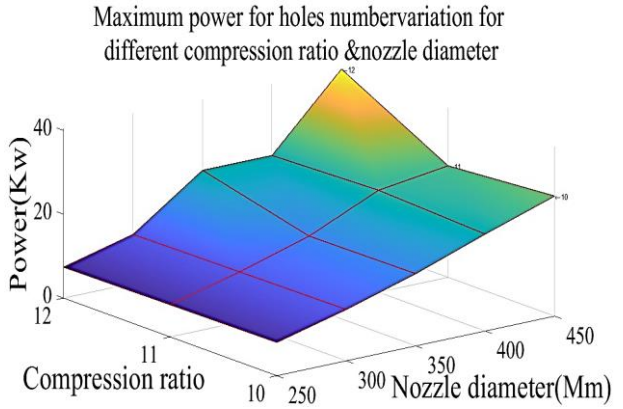

Figure 20. Maximum power for holes number variation for different compression ratio & nozzle diameter.

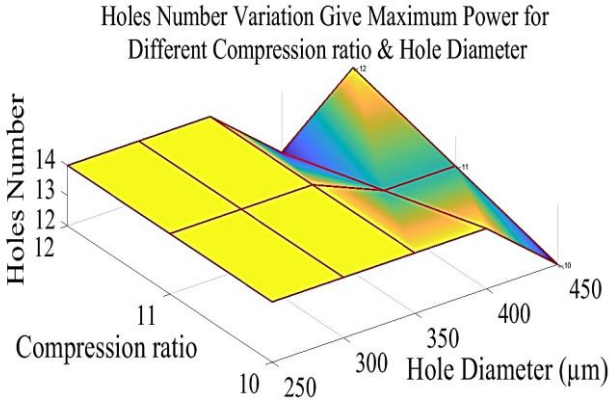

Figure 21. Holes number variation give maximum power for different compression ratio & Nozzle diameter.

4.5 Variation of the Number of Nozzle Holes with Rotation Engine Speed.

Data in the table 2 show the influence of the variation of nozzle diameter number on the maximum values for temperature, pressure, power, heat transfer and emissions. for the mathematical model for a GDI engine at (Rotation Engine speed of 1000, 2000, 3000, 4000, 5000 rpm ,35 MPa injection pressure, compression ratio of 11.5, and spark timing of 140°). The highest of maximum values of temperature, pressure, and emissions were at a rotation engine speed of 1000, and (12) holes. The highest values for maximum power at 4000 rpm and (12) holes, while the highest maximum values for heat transfer are at 5000 rpm and (12) holes.

5. Conclusion

A 4-stroke cycle of a gasoline direct injection engine was mathematically modeled. The mathematical model may be used to analyze the emissions of pollutants from a gasoline direct injection engine as well as its performance. Modeling the combustion with various nozzle hole diameters and numbers was done using the MATLAB algorithm. The following are the key findings from the current investigation.

- Cylinder pressure and temperature were observed to rise as nozzle hole diameter increased, as did maximum peak pressure and burned temperature when nozzle hole diameter was 0.650mm.
- Engine power and heat transfer increased as nozzle hole diameter increased, with a maximum value when nozzle hole diameter was 0.650mm.
- The lowest value of nozzle hole diameter, 0.250mm, was found to have the lowest CO and NO emissions.

Table 2. Variation of Maximum Values Operating Engine Parameters s with Nozzle Holes Number.

Temperature(K)					
	Speed (rpm)				
holes	1000	2000	3000	4000	5000
4	2203	2040	1825	1559	1367
6	2653	2506	2361	1970	1728
8	3087	2984	2883	2372	2057
10	3156	3080	2929	2759	2381
12	3347	3230	3189	3019	2693
Pressure (kPa)					
	Speed (rpm)				
holes	1000	2000	3000	4000	5000
4	7954	7643	5997	5161	4656
6	8198	7892	7704	6453	5695
8	8973	8763	8460	7742	6734
10	9983	9958	9763	9014	7770
12	11019	10943	9987	9597	8805
Power (kW)					
	Speed (rpm)				
Speed rpm/holes	1000	2000	3000	4000	5000
4	7.736	6.364	6.132	5.691	5.16
6	9.133	7.364	11.73	12.5	13.12
8	11.57	14.95	16.53	16.23	17
10	11.3	26.92	20.3	20.93	16
12	10.7	21.58	24.63	45.01	25.62
Heat transfer (kW)					
	Speed (rpm)				
Speed rpm/holes	1000	2000	3000	4000	5000
4	22.97	23.69	24.86	25.91	27.92
6	33.82	35.59	36.95	38.13	38.22
8	44.99	47.35	49.99	50.31	51.49
10	51.42	58.12	59.54	61.47	63.73
12	58.53	70.01	72	74.72	75.95
Mole fraction of CO (Xi)					
	Speed (rpm)				
Speed rpm/holes	1000	2000	3000	4000	5000
4	0.06334	0.004746	0.000341	4.32e-05	8.53e-06
6	0.07814	0.03322	0.005082	0.000828	0.000175
8	0.08852	0.06363	0.02332	0.005306	0.001334
10	0.09082	0.07345	0.09452	0.01744	0.005479
12	0.1049	0.07875	0.06435	0.03249	0.01471
Mole fraction of NO (Xi)					
	Speed (rpm)				
Speed rpm/holes	1000	2000	3000	4000	5000
4	0.02345	0.001616	0.000124	1.69e-05	8.74e-06
6	0.02549	0.01172	0.001729	0.000292	6.5e-05
8	0.02768	0.02338	0.008061	0.001807	0.000465
10	0.03028	0.02504	0.009561	0.005969	0.001865
12	0.3568	0.0258	0.01872	0.01114	0.005018

- When using a nozzle diameter of 0.630 mm and a compression ratio of 11, with nozzle holes ranging from 6 to 12, the maximum power per cycle for the engine was obtained.
- The cylinder pressure and temperature were observed to rise as the number of nozzle holes increased, with 12 nozzle holes producing the highest peak pressure and burned temperature.
- By increasing the number of nozzle holes, up to a maximum of 12, engine power and heat transfer increased.
- With lowest nozzle holes number (four nozzle holes) it was found that CO and NO emissions were the lowest.
- Maximum power per cycle (0.450 mm) and the ideal number of nozzle holes in relation to engine compression ratio with respect to nozzle diameter variation were found to be (14) for nozzle holes and (12) for compression ratio, respectively.
- The highest of maximum values of temperature, pressure, and emissions were at a speed of 1000, and nozzle diameter of 0.650 mm, and (12) holes. The highest values for maximum power at 4000 rpm and nozzle diameter of 0.650 mm and (12) holes, while the highest maximum values for heat transfer are at 5000 rpm, a diameter of 0.65mm and (12) holes.

From the conclusions above, injector parameters (nozzle diameter & holes number) it plays an important role in engine performance and emissions. Knowing the optimal injector parameters and its effect with other parameters on engine performance is necessary. Accordingly, fuel injector must be designed for best engine operation and emissions as low as possible. Therefore, in the future, it is necessary to know the effect of the rest of the parameters, such as fuel injection pressure, engine load, and engine geometry etc., with injector parameters on the performance and emissions of the GDI engine.

Acknowledgements:
The authors are grateful for the assistance they received from the staff at the Mechanical Department of the University of Technology-Iraq.

Nomenclature

a_s	air--fuel ratio	Unit less
A_{inj}	Orifice Area	m²
A_u	unburned area	m²
A_b	Burnt area	m²
Cv	specific heat	kJ/kg.k
C_d	Discharge Coefficient	Unit less
Ca	Area Contraction Coefficient	Unit less
(CR)	compression ratio	Unit less
DQ_1	Convective losses	kW
DQ_2	change in heat transfer	KW
dur_{CA}	Injection Duration	degree
FMEP	Friction mean effective pressure	Pa
hr	radiation heat coefficient	W/m².K
H	Heat transfer coefficient	W/m².K
L	engine's stroke	m

LH V	lower heating values of the provided fuel	kJ/kg
m	mass	Kg
$\dot{m}_f$	Fuel flow rate	kmol/s
$\dot{m}_{CA}$	Fuel flow rate	kmol/deg
MW_f	Molecular weight	kmol/kg
Ns	Rotation Engine Velocity	rpm
Nu_i	Nusselt number	Unit less
P	Pressure	kPs
P_{inj}	Injection Pressure	kPa
P_{injmax}	Maximum Injection Pressure	kPa
P_{injmin}	Minimum Injection Pressure	kPa
Q	overall energy input into the system	kJ
U_{fuel}	Fuel velocity	m/s
ΔU	changing within internal energy	kJ
R	Gas constant	kJ/kg.k
Re	Reynolds number	Unit less
T	Temperature	K
Tw	Wall temperature	K
V	Volume	m³
V_d	Displaced Volume of Engine	m³
W	work output from the system	kJ
$\dot{W}_b$	Brake power	kW
W_i	Work	kJ
$\dot{W}_i$	indicate power	kW
Xb	mass fraction	Unit less

Greek Symbols

Ƞ	combusting efficiency	Unit less
η_m	Mechanic efficiency	Unit less
τ	torque	N.m
γ	Gas index	Unit less
θ	crank angle.	degree
Θ (i)	immediate crank angle	degree
Θ(o)	spark angle at the beginning of combustion	degree
Θ(b)	the burn length	degree
ϕ	equivalence ratio	
ρ_{fuel}	Fuel Density	*kg/m³*

Subscripts

B	burn
U	unburned

Abbreviations

BTDC	Before top dead center
CO	Carbon monoxide
DI	Direct-injection (DI)
Holes	Number of holes in injector
PFI	Port fuel injection
INHNs	Injector nozzle hole numbers
IPs	Fuel injection pressures
GDI	Gasoline direct injecting
NO	Nitrogen monoxide

References:

[1] F. Zhao, M. C. Lai, and D. L. Harrington, "Automotive spark-ignited direct-injection gasoline engines," *Prog. Energy Combust. Sci.*, vol. 25, no. 5, pp. 437–562, 1999, doi: 10.1016/S0360-1285(99)00004-0.

[2] J. Gao, D.-M Jiang, Z.-H Huang, X.-B Wang, "Numerical Study on Spray and Mixture Stratified Combustion in a Direct Injection Gasoline Engine," *Chinese Society for Internal Combustion Engines.*, vol 23 (4), pp. 297-306, 2005

[3] M. A. Mashkour, "Investigation of Spark Ignition Engine Mathematical Model Using MATLAB (GUI)," *Advances in Natural and Applied Sciences.* vol 11 (11) ,pp 36-50, 2017, [Online]. Available: http://www.aensiweb.com/ANAS.

[4] R. Sharma, "Experimental study of the Effect of Fuel Injector nozzle holes on Direct Injection Diesel Engine," *IOSR J. Mech. Civ. Eng*., vol. 7, no. 4, pp. 67–74, 2013, doi: 10.9790/1684-0746774.

[5] Y. J. C. and C. H. J. B. H. LEE, J. H. SONG, "Effect of The Number of Fuel Injector Holes on Characteristics of Combustion and Emissions in A Dlesel Engine," *Int. J. Automot. Technol*., vol. 11, no. 6, pp. 783–791, 2010, doi: 10.1007/s12239.

[6] M. Vijay Kumar, A. Veeresh babu, P. Ravi Kumar, and T. Manoj Kumar Dundi, "Influence of different nozzle hole orifice diameter on performance, combustion and emissions in a diesel engine," *Aust. J. Mech. Eng*., vol. 18, no. 2, pp. 179–184, 2020, doi: 10.1080/14484846.2018.1453975.

[7] C. Jiang, M. C. Parker, J. Helie, A. Spencer, C. P. Garner, and G. Wigley, "Impact of gasoline direct injection fuel injector hole geometry on spray characteristics under flash boiling and ambient conditions," *Fuel*, vol. 241, no., pp. 71–82, 2019, doi: 10.1016/j.fuel.2018.11.143.

[8]M. B. Ahmed and M. W. Mekonen, "Effects of Injector Nozzle Number of Holes and Fuel Injection Pressures on the Diesel Engine Characteristics Operated with Waste Cooking Oil Biodiesel Blends," *Fuels*, vol. 3, no. 2, pp. 275–294, 2022, doi: 10.3390/fuels3020017.

[9] A. A. Reddy and J. M. Mallikarjuna, "Parametric Study on a Gasoline Direct Injection Engine - A CFD Analysis," *SAE Tech.*, Paper no 2017-26-0039, 2017, doi: 10.4271/2017-26-0039.

[10] P. D. Jadhav and J. M. Mallikarjuna, “Effect of fuel injector hole diameter and injection timing on the mixture formation in a GDI engine - A CFD study,” *Int. J. Comput. Methods Exp. Meas*., vol. 6, no. 4, pp. 737–748, 2018, doi: 10.2495/CMEM-V6-N4-737-748.

[11] J. B. Heywood, *Internal Combustion Engine Fundamentals*. N. York: McGraw-Hill , pp. 389–716, 1988

[12] Y. G. Guezennec and W. Hamama, “Two-zone heat release analysis of combustion data and calibration of heat transfer correlation in an I. C. engine,” *SAE Tech.* Paper., no. 724, 1999, doi: 10.4271/1999-01-0218.

[13] G. P. Blair, *The Basic Design of Two-Stroke Engines,*USA. Society of Automotive Engineers, Inc 400 commonwealth engine, pp.205-297, 1990 doi: 10.4271/r-104.

[15] W. J. D. Annand, “Heat Transfer in The Cylinders of Reciprocating Internal Combustion Engines,” *Thermodynamics and Fluid Mechanics Group*, vol. 177, no. 36, pp. 973–996, 1963, doi: 10.1243/PIME.

[16] D. L. Siebers, “Scaling liquid-phase fuel penetration in diesel sprays based on mixing-limited vaporization,” *SAE Tech.* Paper, no. 724, 1999, doi: 10.4271/1999-01-0528.

[17] C. R. F. A. T. Kirkpatrick, *Internal Combustion Engines Applied Thermosciences*, 3rd ed., John Wiley & Sons, Ltd, pp.84-120, 2016.

[18] C. Olikara and G. L. Borman, “A computer program for calculating properties of equilibrium combustion products with some applications to I.C. engines,” *SAE Tech*. Paper no 750468., 1975, doi: 10.4271/750468.

[19] G. L. B. R. B. Krieger, *The computation of apparent heat release for internal combustion engines.* New York: ASME, pp66-WA/DGP-4 1966.